# Waveguide-type all-NbN SIS mixers on MgO substrates

Masanori Takeda[1], Yoshinori Uzawa[1], Akira Kawakami[1], Zhen Wang[1], and Takashi Noguchi[2]
[1]Kansai Advanced Research Center, National Institute of Information and Communications Technology
[2]Nobeyama Radio Observatory, National Astronomical Observatory of Japan
E-mail: takeda@po.nict.go.jp

**Abstract**

We present the first experimental results on waveguide-type all-NbN SIS receivers fabricated on MgO substrates designed in a frequency range from 780 to 960 GHz. The receiver has a resonant distributed SIS junction one wavelength long at 870 GHz as the tuning circuit and a diagonal feed horn. The mixer chip was fabricated with accuracies of less than 10 μm in width and +/- 5 μm in thickness by optimizing the cutting and polishing conditions for MgO substrates and was successfully mounted in a waveguide-mixer block. Using a conventional Y-factor method for receiver-noise measurement, a minimum DSB receiver-noise temperature of 700 K was obtained at an LO frequency of 770 GHz. The contribution to noise made by the input system was dominant in receiver noise and the input-noise temperature was more than 300 K over the measured band.

## 1. Introduction

The Atacama Large Millimeter Array (ALMA) requires superconductor-insulator-superconductor (SIS) receivers with ultra-low noise performance [1]. ALMA receivers cover a frequency range from 30 to 960 GHz, which is divided into ten bands. The highest (band 10) is in a frequency range from 787 to 960 GHz. Although Nb-based SIS receivers have achieved excellent performance below a gap frequency of 700 GHz [2, 3], it is well known that receiver-noise temperature rapidly degrades above the gap frequency. The major loss component is in Nb microstrips. Therefore, band-10 receivers require their microstrips to be fabricated using high-gap materials such as NbN and NbTiN. Additionally, there is a real need for SIS receivers to involve waveguide coupling techniques in the ALMA.

Single-crystal NbN films fabricated on MgO substrates have a high superconducting critical temperature of 16.5 K, which corresponds to a gap frequency of about 1.4 THz. Also, the tunnel junctions are able to be fabricated using MgO or AlN tunnel barriers [4, 5]. This indicates that NbN-based SIS receivers offer the possibility of low-noise operation to at least 1.4 THz. Actually, good mixing properties have been obtained in SIS receivers with quasi-optical coupling techniques [6, 7]. Following these encouraging results, we have developed waveguide-type all-NbN SIS mixers fabricated on MgO substrates for the band-10 ALMA.

However, the waveguide-mixer chip must be reduced in size because MgO has a relatively large dielectric constant ($\varepsilon \sim 9.6$), and it is extremely difficult to cut and polish the MgO substrate compared to its quartz and silicon counterparts because MgO has strong cleavage properties. Therefore, some technical solutions are needed for the waveguide mixer. These are to reduce the cutting-edge chipping that occurs in cutting the MgO substrate, control the substrate thickness in polishing and chip handling, and mount the extremely small mixer chip into the mixer block. In this paper, we describe the design of the waveguide mixer, the method used to fabricate the mixer chip, and the experimental results of receiver-noise measurements.

## 2. Mixer design

### *2.1 Waveguide mixer*

The design of the waveguide input circuit including the RF choke was done using Ansoft's High Frequency Structure Simulator (HFSS version 9), which has a finite-element method incorporated [8]. The dielectric constant of the MgO substrate was assumed to be 9.6. The center frequency was set to 870 GHz, which is the center frequency for band-10 ALMA. The schematic layout for the waveguide input circuit is in Fig. 1. The aperture of the substrate channel is 0.074 x 0.074 mm and the mixer chip is 1-mm long, 0.064-mm wide, and 0.025-mm thick. We chose a half reduced-height waveguide with dimensions of 0.265 x 0.065 mm as the input waveguide and the length

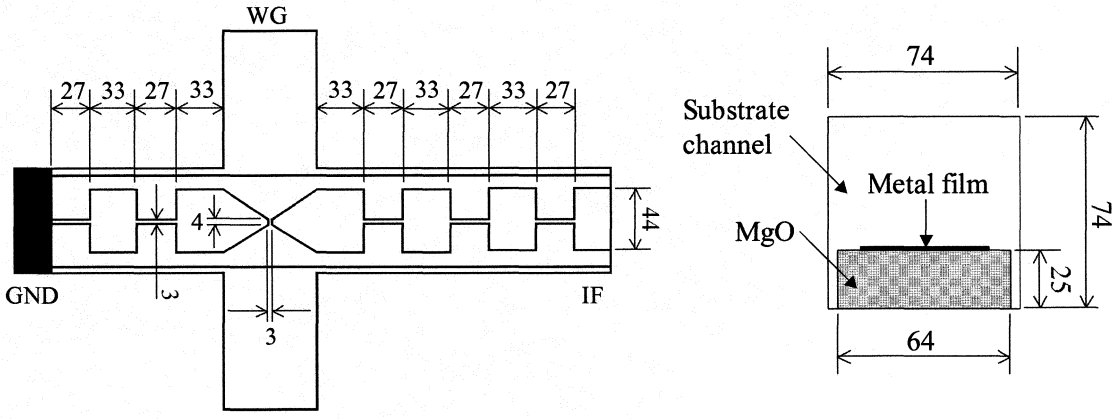


Fig. 1 Schematic layout of waveguide input circuit with MgO substrate. All dimensions are in μm. Mixer chip is 1-mm long, 0.064-mm wide, and 0.025-mm thick.

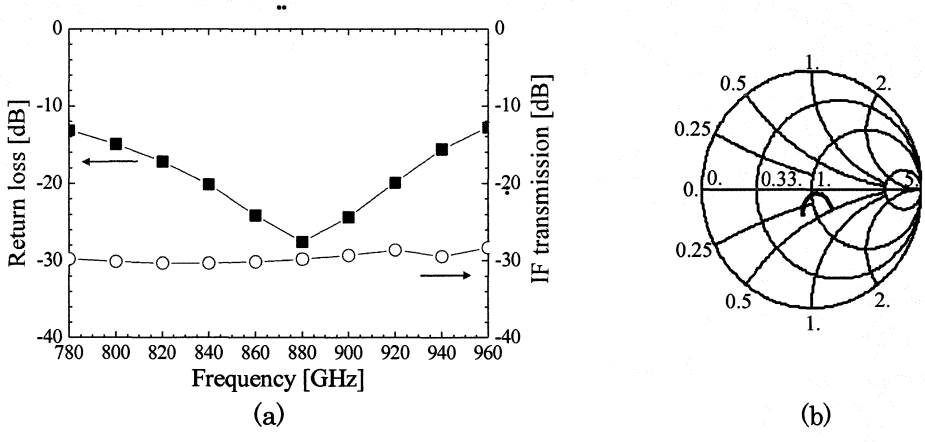


Fig. 2 (a) Return-loss characteristic at feed point and IF transmission characteristics to IF port. (b) Impedance Smith chart at feed point normalized to 60 Ω.

of the backshort cavity was 0.021 mm. We determined the optimum backshort position so that the calculated return losses were minimized in the frequency range of interest. The feed point was set to the center of the bow-tie probe.

Figure 2(a) plots the return-loss characteristic of the RF signal at the feed point and the transmission characteristics to the IF port. The return loss was less than -10 dB in a frequency range from 780 to 960 GHz. The transmission of the RF signal to the IF port is less than -28 dB and the RF signal was not considered to have leaked to the IF port The impedance Smith chart at the feed point normalized to 60 Ω is in Fig. 2(b). The feed point impedance was set to 60 Ω from this Smith chart.

To evaluate the tolerances of variations in width and thickness, we calculated the dependence of return-loss characteristics on variations. Figure 3(a) plots the return loss at a substrate width of 0.054 mm and 3(b) plots the return losses at thicknesses of 0.02 and 0.03 mm. We can see from these figures that a variation of a few microns changes the characteristics dramatically. Therefore, the mixer chip must be fabricated within accuracies of 10 μm in cutting and +/- 5 μm in polishing the MgO substrate.

We choose a diagonal horn with an aperture of 2.5 x 2.5 mm as the feed horn. A diagonal horn is easy to machine and has good beam efficiency in the E- and H-planes [9].

*2.2 Tuning circuit*

In general, the reactance of an SIS mixer due to its large geometrical capacitance must be removed by adding an appropriate tuning circuit to efficiently feed the signal to the junction. Distributed mixing using nonlinear SIS

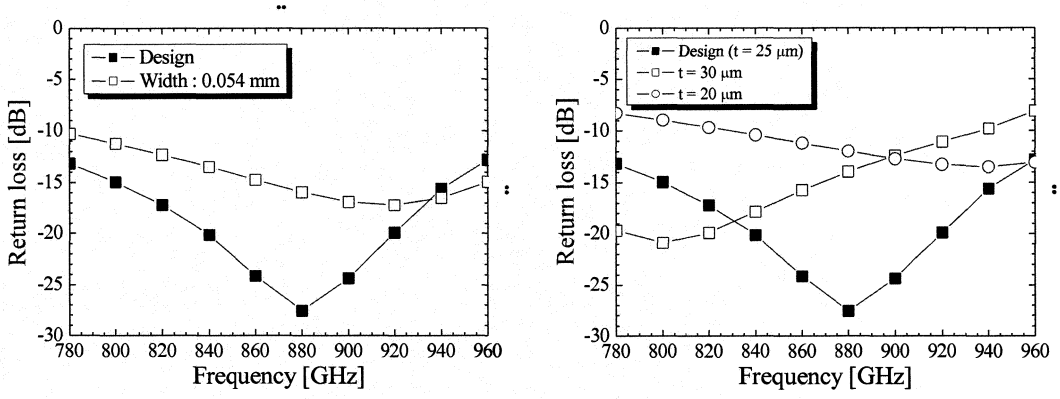


Fig. 3 Variations in return-loss characteristics due to dimensional change in substrate: (a) return-loss characteristics at widths of 0.064 mm (design) and 0.054 mm. (b) return-loss characteristics at thicknesses of 0.025 mm (design), 0.03 mm, and 0.02 mm.

transmission lines have demonstrated low noise and good tunability at submillimeter wavelengths [10-12]. We adopted a resonant distributed SIS mixer as the tuning circuit. The resonant distributed SIS junction consisted of an NbN/MgO/NbN tunnel junction and an NbN/MgO/NbN microstrip as we can see from Fig. 4(a). A 0.6-μm-wide SIS junction with a symmetrical counter-electrode overhang of 1 μm on either side was assumed. The critical current density of the junction was set to 20 kA/cm$^2$. Also, the junction specific capacitance was assumed to be 145 fF/μm$^2$ and the $I_cR_n$ product was assumed to be 3.8 mV. The input impedance of the resonant distributed SIS junction at 870 GHz is plotted as a function of its length in Fig. 4(b). We found that an open long SIS junction becomes a resonator when its length equals integer multiples of $\lambda_g/2$. We chose a full-wave resonant distributed SIS junction with a junction length of 7 μm taking the tuning bandwidth and moderate input impedance into consideration. The input impedance of the junction was matched the feed point through a $\lambda_g/4$-microstrip transformer.

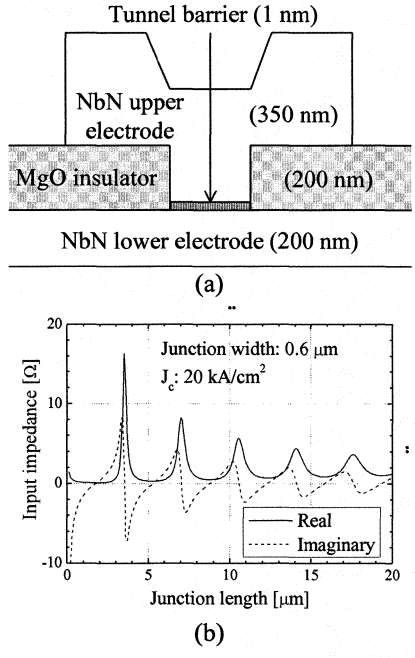


Fig. 4 (a) Schematic layout of distributed NbN SIS junction. (b) Input impedance of distributed junction as a function of junction length at 870 GHz for 0.6-μm-wide junction with symmetrical counter-electrode overhang of 1 μm on either side.

### 3. Mixer fabrication

The epitaxial NbN/MgO/NbN trilayers that formed the tunnel junctions were deposited *in situ* on single-crystal (100) MgO substrates 15-mm square and 0.3 mm in thickness at ambient temperature. The base and counter NbN electrodes of the tunnel junctions were deposited by reactive dc-magnetron sputtering. The MgO tunnel barrier was deposited by rf sputtering. The base and counter NbN were each 200 nm thick. The critical current density was controlled by the thickness of the MgO barrier. The bow-tie waveguide probe was formed with conventional photolithography and reactive etching (RIE). Then an SIS-junction mesa was formed using photolithography and RIE. After a 200-nm-thick MgO film was deposited by rf- and dc-magnetron sputtering to electrically insulate the base electrode and contact-wiring layer, the photoresist was lifted off. Finally, a 350-nm-thick NbN film was deposited and the wiring layer and transformer were defined by photolithography and RIE.

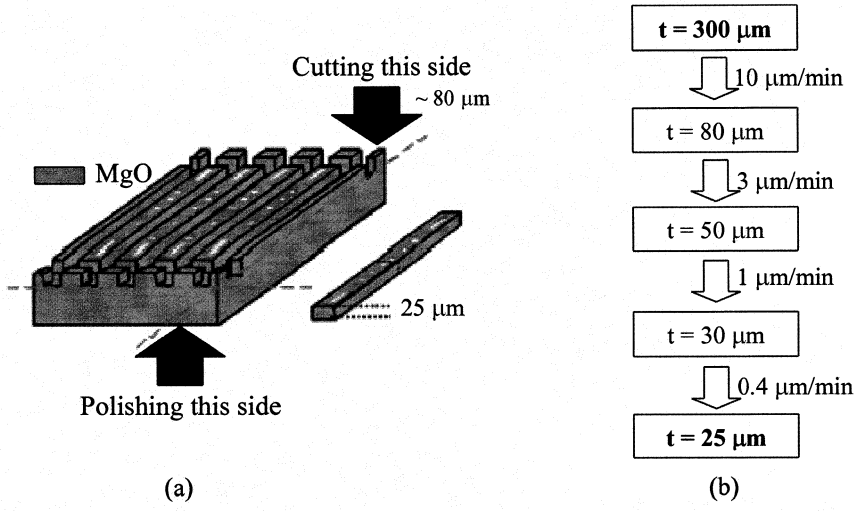


Fig.5 (a) Fabrication of mixer chip. MgO substrate is first cut to depth of 80 μm from surface, and then its backside is polished down to thickness of 25 μm. (b) Polishing process for MgO substrate. Polishing rate is changed by replacing diamond lapping film.

After the fabrication process was completed, the MgO substrate was first cut to a depth of 80 μm from the surface with a (DISCO) dicing machine (Fig. 5(a)). In general, the tip of the blade is rounded. Therefore, we cut more deeply than the design thickness using a narrow blade with a thickness of 25 μm (NBC-Z1050) so that the shape of blade did not appear in the cutting plane. In dicing, the MgO had larger cutting-edge chipping than either quartz or silicon. Although the amount of chipping in quartz and silicon substrates is several microns, it is more than several tens of microns in MgO substrate if cutting is done under the same conditions. Chipping is a serious problem in defining the width of the mixer chip with sufficient accuracy. By optimizing dicing conditions and doing appropriate pre-cutting, we were able to reduce the chipping to around 3 μm using an NBC-Z1050 blade.

The cut substrate was glued upside down on a dedicated plate and its backside was then polished down to a design thickness of 25 μm using a lapping machine. The polishing was started with a diamond lapping film that had rough grain. We then lowered the polishing rate by replacing the lapping film with one that had finer grain and by reducing the speed the stage rotated at. Finally, polishing could be done with sufficient accuracy at a rate of 0.4 μm/min. We confirmed that the final thickness was accurate within 5 μm with both a micrometer and an optical microscope. The process of polishing is outlined in Fig. 5(b).

The fabricated mixer chip was mounted into the waveguide mixer block. However, the pressure bonding with indium metal was very difficult because the substrate was very thin. We first bonded the mixer chip with an adhesive (crystal bond 509) that was acetone soluble. Then, both ends of the mixer chip were directly connected to a 50-Ω microstrip and the mixer block with 18-μm-diameter aluminum wires to extract the IF output and to supply the DC bias. The bend in the substrate becomes much more pronounced as the substrate gets thinner, and could lead to breakage during mounting. In fact, we observed a large bend in our mixer chip. However, the substrate seldom broke

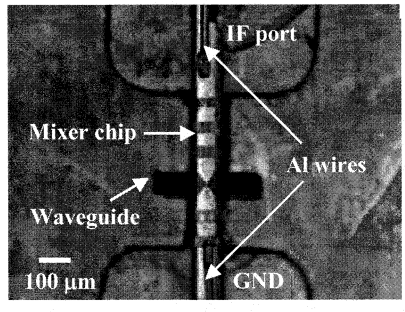


Fig. 6 Optical micrograph of mixer chip installed into substrate channel in waveguide mixer block.

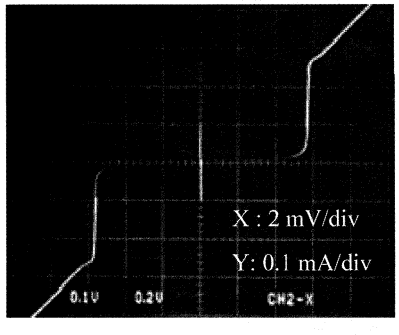


Fig. 7 Current-voltage characteristic of epitaxial NbN SIS mixer at 4.2 K. The horizontal scale is 2 mV per division, and the vertical scale is 0.1 mA per division.

when mounting with this method. Figure 6 is an optical micrograph of the mixer chip installed into a slot on the inside of the mixer block. The dc I-V characteristics of the mounted mixer chip are plotted in Fig. 7. The cutting and polishing processes did not affect the I-V characteristics, as far as the gap voltage, the leakage current, and the normal-state resistance were concerned. Additionally, the characteristics did not change for some heat cycles between room temperature and 4.2 K. However, the critical current density of the fabricated mixer was about 2.6 kA/cm$^2$, which is considerably less than the design value. An extremely small sub-gap leakage current and strong nonlinearity were observed in the I-V characteristics, where the ratio of sub-gap resistance at 4.0 mV to normal-state resistance was around 18 at 4.2 K.

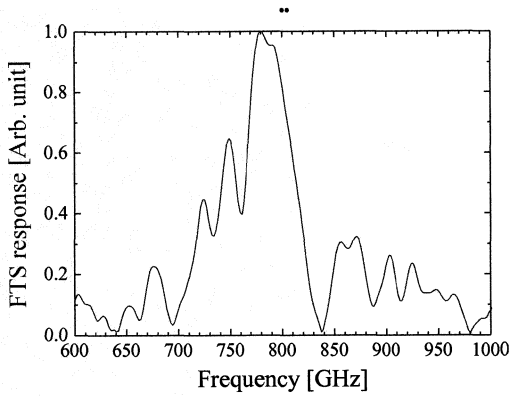


Fig. 8 FTS response of mixer as a function of frequency.

**4. Receiver-noise measurements**

The receiver response as a function of frequency was measured with a Fourier transform spectrometer (FTS) using the fabricated mixer as a direct detector prior to estimating the receiver-noise temperature. The FTS consisted of a Martin-Puplett interferometer using wire grids as polarizers and an Hg arc lamp as a broadband radiation source. The mixer was cooled by liquid He in a cryostat and was placed in front of the Teflon window of the FTS. The FTS response was directly related to the input coupling efficiency of the RF signal to the mixer. It is well known that the shape of FTS response as a function of frequency is strongly correlated to the receiver-noise temperature as a function of frequency and that minimum receiver-noise temperature can be obtained at a frequency where a maximum peak is observed for FTS response. The FTS response of the mixer is plotted in Fig. 8. We can see from the FTS data that the 3-dB bandwidth ranges from 760 to 810 GHz and low-noise temperature can be obtained in that frequency range. The best noise temperature can be expected at a frequency of around 780 GHz. Although the designed center frequency was 870 GHz, the measured center frequency shifted lower. This was because the dimensions of the fabricated junction were different from that designed. This is especially as fabrication error in the counter-electrode overhang severely affects center frequency, and a smaller overhang contributes to a lower center frequency. Additionally, the ratio of the spectrum of interest to its sideband was very small, i.e., the S/N ratio was very poor. This will create large input losses including the matching loss between the feed point and the junction in measuring the receiver-noise temperature.

The noise temperature of the receiver was estimated with the conventional Y-factor method using blackbody radiation on 295- and 77-K loads as the RF signal source. The RF signal was quasi-optically coupled to the LO signal from a backward-wave oscillator (BWO) through a 9-μm-thick Mylar film used as a beam splitter and this was guided to the mixer block cooled to 4.2 K through a 0.5-mm-thick Teflon vacuum window and a diagonal feed horn. A permanent magnet was attached to the sidewall of the mixer block to suppress the Josephson current. The IF output signal was first amplified with a high electron-mobility transistor (HEMT) amplifier with a bandwidth of 500 MHz centered at 1.5 GHz through an isolator at 4.2 K, and then amplified with a room-temperature post-amplifier. The IF signal was finally fed to a power meter. No corrections were made for the losses in front of the receiver.

Figure 9 plots the IF-output-power characteristics to hot and cold loads, along with the dc I-V characteristics with and without LO power at the 770 GHz of the receiver as a function of bias voltage. When LO power was applied, photon-assisted tunneling steps could clearly be observed. In terms of I-V characteristics, the lowered gap voltage compared with that in Fig. 7 is due to the strong magnetic

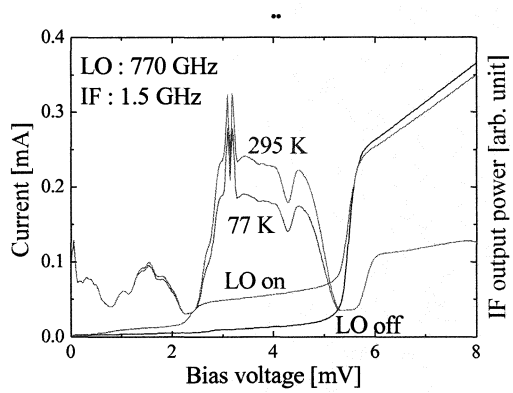


Fig. 9 Measured dc current-voltage characteristics of mixer with and without LO at 770 GHz. Also shown is receiver IF output power as a function of bias voltage for hot (295 K) and cold (77 K) loads.

field. A maximum Y-factor of 1.28 was obtained at a bias voltage of 4 mV, and this provides a double sideband (DSB) receiver-noise temperature of 700 K. Shot-noise calibration [13] yielded IF system noise of about 5 K and mixer conversion loss of about 12 dB, including losses in the optics and beam splitter. The poor input coupling efficiency was considered to be the cause of the large conversion loss.

Figure 10 plots the receiver-noise temperature as a function of LO frequency. The narrow bandwidth is due to the low critical-current density of the fabricated junction. The receiver-noise temperature was very large over the measured band. To find the cause of the large noise temperature, we compared it with that obtained with an SIS mixer using quasi-optical coupling. The quasi-optical SIS mixer consisted of a 3-mm-radius MgO hyperhemispherical lens with a 50-μm-thick Kapton-JP antireflection cap and a single-crystal twin-slot antenna. A resonant distributed SIS junction was also adopted in the quasi-optical mixer as the tuning circuit. The dimensions of the junction and $\lambda_g/4$-microstrip transformer in the quasi-optical mixer were the same as those for the waveguide mixer. Since the quasi-optical and waveguide mixer were arranged on the same photomask, both had the same critical-current density of 2.6 kA/cm$^2$. The receiver-noise temperature in the quasi-optical mixer is also plotted in Fig. 10. It was less than 400 K (DSB) in a frequency range from 762 to 810 GHz and a minimum noise temperature of 278 K, which is about seven times larger than the quantum limited noise, obtained at an LO frequency of 788 GHz. The receiver noise in the waveguide mixer was more than twice that in the quasi-optical mixer. From this, we considered that the large receiver noise in the waveguide mixer was due to losses originating between the horn and feed point, rather than matching loss between the feed point and junction. Actually, the input-noise temperature was more than 300 K in the measured band. The waveguide losses due to a roughness of the inside wall of the waveguide and RF leakage due to undesirable higher RF-signal modes in the substrate channel were considerable factors. If the higher RF-signal modes in the substrate channel are the main cause, the receiver noise can be reduced by making the substrate thinner and redesigning the waveguide input circuit.

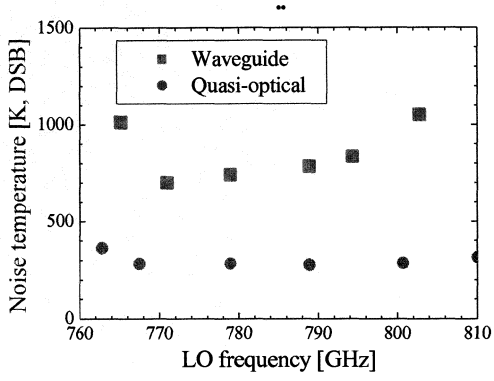


Fig. 10 Receiver-noise temperatures of waveguide and quasi-optical mixers as a function of frequency.

## 5. Summary

We are developing waveguide-type all-NbN SIS mixers on MgO substrates for the band-10 ALMA. The mixer chip we designed was able to be fabricated within an accuracy of 6 μm in width and 5 μm in thickness by optimizing the dicing and polishing conditions. The dicing and polishing processes did not affect the dc I-V characteristic of the fabricated mixer. Additionally, the characteristics did not change during some heat cycles between room temperature and 4.2 K. The micro mixer-chip was able to be successfully installed into a substrate channel in a waveguide mixer block and the receiver performance was estimated with FTS and heterodyne measurements. The minimum noise temperature of the receiver was 700 K (DSB) at an LO frequency of 770 GHz. The large input losses, especially in the waveguide input circuit, were the cause of the poor receiver performance. We believe that receiver performance can be improved by redesigning the waveguide input circuit.

## References

[1] http://www.alma.nrao.edu/

[2] J. W. Kooi, M. Chan, B. Bumble, H. G. LeDuc, P. Schaffer, and T. G. Phillips, "230 and 492 GHz low noise SIS waveguide receivers employing tuned Nb/AlOx/Nb tunnel junctions", *Int. J. Infrared Millim. Waves*, Vol. 16, No. 12, pp. 2049-2068, 1995.

[3] C. E. Tong, R. Blundell, S. Paine, D. C. Papa, J. Kawamura, X. Zhang, J. A. Stern, and H. G. LeDuc, "Design and characterization of a 250-350 GHz fixed-tuned superconductor-insulator-superconductor receiver", *IEEE Trans. Microwave Theory Tech.*, Vol. 44, No. 9, pp. 1548-1556, 1996.

[4] Z. Wang, A. Kawakami, Y. Uzawa, and B. Komiyama, "NbN/AlN/NbN tunnel junctions fabricated at ambient substrate temperature", *IEEE Trans. Appl. Supercond.*, Vol. 5, No. 2, pp. 2322-2325, 1995.

[5] A. Kawakami, Z. Wang, and S. Miki, "Fabrication and characterization of epitaxial NbN/MgO/NbN Josephson tunnel junctions", *J. Appl. Phys.*, Vol. 90, No. 9, pp. 4796-4799, 2001.

[6] Y. Uzawa, M. Takeda, A. Kawakami, and Z. Wang, "A tuning circuit with two half-wave distributed junctions for all-NbN SIS mixers", *Int. J. Infrared Millim. Waves*, Vol. 24, No. 10, pp. 1749-1757, 2003.
[7] A. Kawakami, Y. Uzawa, and Z. Wang, "Development of epitaxial NbN/MgO/NbN-superconductor-insulator-superconductor mixers for operations over the Nb gap frequency", *Appl. Phys. Lett.*, Vol. 83, No. 19, pp. 3954-3956, 2003.
[8] *High Frequency Structure Simulator*, Ansoft Co., Four Station Square Suite 200, Pittsburgh, PA 15219, USA.
[9] S. Withington and J. A. Murphy, "Analysis of diagonal horns through Gaussian-Hermite modes", *IEEE Trans. Antennas Propagat.*, Vol. 40, No. 2, pp. 198-206, 1992.
[10] V. Yu. Belitsky and E. L. Kollberg, "Superconductor-insulator-superconductor tunnel strip line: Features and applications", *J. Appl. Phys.*, Vol. 80, pp. 4741-4748, 1996.
[11] T. Matsunaga, C. E. Tong, R. Blundell, and T. Noguchi, "A 600-700 GHz resonant distributed junction for a fixed-tuned waveguide receiver", *IEICE Trans. Electron.*, Vol. E85-C, pp. 738-741, 2002.
[12] Y. Uzawa, A. Kawakami, S. Miki, and Z. Wang, "Performance of all-NbN quasi-optical SIS mixers for the terahertz band", *IEEE Trans. Appl. Supercond.*, Vol. 11, No. 1, pp. 183-186, 2001.
[13] D. P. Woody, R. E. Miller, and M. J. Wengler, "85-115-GHz receivers for radio astronomy", *IEEE Trans. Microwave Theory Tech.*, Vol. 33, pp. 90-95, 1985.

**Acknowledgments**

We would like to thank Dr. C. E. Tong of the Harvard-Smithsonian Center for Astrophysics for his invaluable comments. We also wish to thank Dr. S. Saito of the National Institute of Information and Communications Technology for his technical assistance in testing the FTS measurements. This work was supported in part by the ALMA Joint Research Fund by the National Astronomical Observatory of Japan.